

Observation of a “Ridge” correlation structure in high multiplicity proton-proton collisions: A brief review

WEI LI

*Laboratory of Nuclear Science, Department of Physics,
Massachusetts Institute of Technology, 77 Massachusetts Avenue,
Cambridge, MA 02139, USA
davidhw@mit.edu*

Received 8 May 2012

Revised 30 May 2012

This paper briefly reviews the striking experimental observation of a ridge-like dihadron correlation structure in high multiplicity proton-proton collisions at the Large Hadron Collider (LHC). Recent progress of both experimental and theoretical efforts on understanding the physical origin of the novel effect is reviewed. Outlook on future direction of possible new studies is discussed.

Keywords: ridge; high multiplicity; long-range; near-side

PACS numbers: 25.75.Gz, 12.38.Qk, 25.75.Ld

1. Introduction

The observation of a novel long-range dihadron correlation in very high multiplicity proton-proton (pp) collisions by the Compact Muon Solenoid (CMS) collaboration¹ at the Large Hadron Collider (LHC) opened up the door to a variety of frontiers in the crucial non-perturbative phenomena of Quantum Chromodynamics (QCD) at a very high density regime. The new finding describes a novel correlation that particles coming out of the collision are aligned in their azimuthal angle (ϕ) over a large pseudorapidity (η) gap ($\eta = -\ln[\tan(\theta/2)]$ and θ is the polar angle relative to the beam direction). This “ridge”-like structure is found to be absent in minimum bias events but emerges as particle multiplicity reaches very high values. This phenomenon has not been observed before in proton-proton (pp) collisions but resembles similar effects seen in collisions of heavier nuclei such as copper and gold ions at the Relativistic Heavy Ion Collider (RHIC). Therefore, wide interests have been aroused in both the high energy particle and nuclear physics community.

The motivation of studying very high multiplicity hadron production processes is many-sided. High multiplicity events are rare in nature and dominated by significant non-perturbative QCD activities. Potential new phenomena of QCD could be revealed, and thus warrant detailed investigations. Furthermore, with increas-

ing collision rate at the highest center of mass energy pp collisions at the LHC, the tail of the multiplicity distribution is typically reaching values as high as more than 50 charged particles per unit pseudorapidity. Such high particle density begins to approach that of semi-peripheral collisions of relativistic nuclei such as copper at RHIC ². Therefore, it is natural to search for the possible signatures of high-density and hot QCD matter, known as the “Quark-Gluon Plasma” (QGP), in a high multiplicity pp environment. The QGP is believed to form in relativistic heavy ion collisions with fascinating properties such as close-to-zero shear viscosity over entropy density ratio and extremely high opacity ^{3,4,5,6}.

This review is organized as follows: the experimental observation of the ridge effect in high multiplicity pp collisions at the LHC is first summarized in Section 2. A brief review of similar phenomena in relativistic heavy ion collisions is provided in Section 3. Various theoretical interpretations are described in Section 4. In the end, a summary and outlook on future directions of possible new studies in order to advance our understanding of the ridge is discussed in Section 5.

2. Observation of the “Ridge” in high multiplicity proton-proton interactions

Experimentally, seeking for new phenomena in high multiplicity pp collisions is a demanding task. In particular, high-intensity proton beams are colliding at the LHC with extremely high rate. The key challenge is to identify and record collisions with large number of particles originating from a single primary vertex and avoid events from multiple low multiplicity pp collisions (pileups). The powerful High-Level Trigger farm in CMS ensures the prompt online reconstruction of charged particle trajectories using three layers of silicon pixel detector with high resolution in momentum (a few %) and back pointing position (~ 100 microns) such that all primary reaction vertices can be precisely located in each bunch crossing. A display of a very high multiplicity pp event recorded in CMS is illustrated in Fig. 1, with more than 200 charged particles produced from a single primary vertex. A pp data sample corresponding to an integrated luminosity of about 1 pb^{-1} was used for the first novel observation. About 350,000 single-vertex high multiplicity pp events having average multiplicity 7–8 times that of minimum bias collisions were recorded. These kind of high multiplicity events are produced with a probability of only 10^{-5} – 10^{-6} .

Studies of multi-particle correlations in pp collisions provide the detailed information on the properties of particle production beyond single-particle inclusive yield measurement. The technique of dihadron angular correlations essentially reconstructs an image of the event structure in the phase space. Fig. 2a shows a transverse momentum (p_T) inclusive dihadron angular correlation function as a function of the relative pseudorapidity ($|\Delta\eta| = |\eta_1 - \eta_2|$) and azimuthal angle ($|\Delta\phi| = |\phi_1 - \phi_2|$) in minimum bias pp collisions at the center-of-mass energy (\sqrt{s}) of 7 TeV for all charged particles with $p_T > 0.1 \text{ GeV}/c$, measured by the CMS ex-

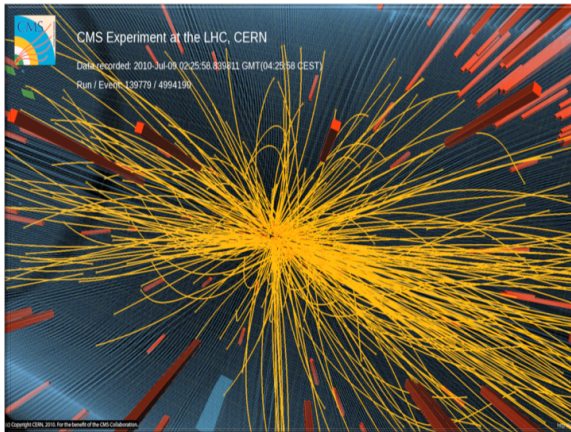


Fig. 1: Event display of a single-vertex high multiplicity pp event at $\sqrt{s} = 7$ TeV recorded by the CMS experiment, where there are more than 200 charged particles produced.

periment at the LHC ¹. The analysis procedure was established in Refs. 7, 8, 9. The dihadron correlation function is defined as follows:

$$R(\Delta\eta, \Delta\phi) = \left\langle \left(\langle N \rangle - 1 \right) \left(\frac{S_N(\Delta\eta, \Delta\phi)}{B_N(\Delta\eta, \Delta\phi)} - 1 \right) \right\rangle_{bins}, \quad (1)$$

where the signal $S_N(\Delta\eta, \Delta\phi)$ denotes the charged particle pair density and the background $B_N(\Delta\eta, \Delta\phi)$ is given by the distribution of uncorrelated particle pairs constructed using the event-mixing technique. Finally, $R(\Delta\eta, \Delta\phi)$ is found by averaging over all event multiplicity bins, N . The two-dimensional (2-D) structure in Fig. 2a exhibits a variety of features. A narrow peak at $(\Delta\eta, \Delta\phi) \sim (0,0)$ is originated from higher p_T hard processes like jets; An approximately Gaussian structure at $\Delta\eta \sim 0$ (near side) extending over the whole range of $\Delta\phi$ arises from the decay of clusters with lower p_T (e.g., soft QCD string fragmentation); In addition, an elongated structure (also like a ridge) at $\Delta\phi \sim \pi$ (away side) spreading over a broad range in $\Delta\eta$ can be interpreted as due to back-to-back jets or more generally momentum conservation.

The p_T -integrated dihadron correlation function in high multiplicity pp events, shown in Fig. 3a, shares a similar structure to that for minimum bias events (Fig. 2a). Besides the more pronounced away-side correlations due to jettier environment (selection on high multiplicity naturally biases toward events containing higher E_T jets and enhances the back-to-back correlations), nothing appears to be unexpected. Striking phenomena emerges if one not only raises the event multiplicity but also varies the transverse momenta of particles. In the intermediate p_T range (1–3 GeV/c) shown in Fig. 3b, a striking “ridge”-like structure appears at $\Delta\phi \sim 0$ extending to $|\Delta\eta|$ of at least 4 units. The ridge is approximately flat in $\Delta\eta$ and also

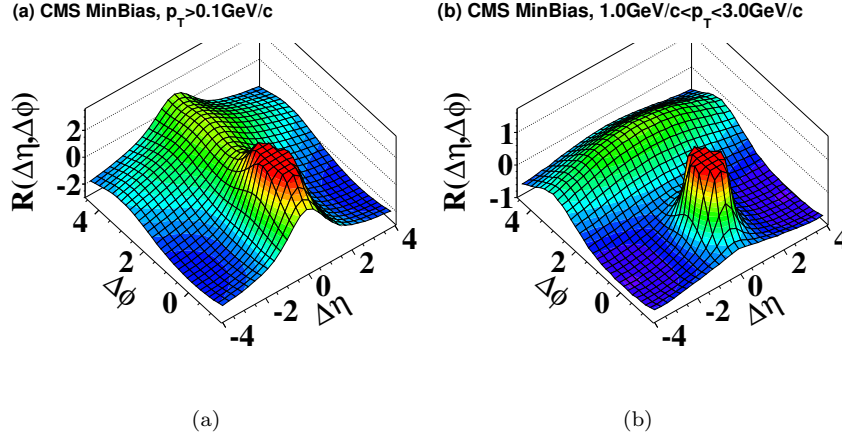


Fig. 2: 2-D dihadron correlation functions for minimum bias pp collisions at $\sqrt{s} = 7$ TeV (a) with $p_T > 0.1$ GeV/c and (b) with $1 < p_T < 3$ GeV/c measured by the CMS experiment ¹.

found to have no dependence on the charge sign of particles (Fig. 10 in Ref. 1). Same effect can also be observed when correlating an inclusive photon (mostly from π^0 decay) with a charged hadron or another inclusive photon ¹. This novel feature of the data has never been seen in dihadron correlation measurements of pp collisions or MC generators before.

Following up the first observation of the ridge in high multiplicity pp collisions, the detailed studies of ridge properties as a function of event multiplicity, transverse momentum and pseudorapidity gap were carried out ^{10,11}. The analysis was performed not only for two particles selected from the same p_T range as was done in Ref. 1, but also for one trigger particle within a specific p_T^{trig} range associated with another particle within a specific p_T^{assoc} range. The p_T^{trig} and p_T^{assoc} can be identical or different. The per-trigger-particle associated pair yield distribution, $\frac{1}{N_{\text{trig}}} \frac{d^2 N^{\text{pair}}}{d\Delta\eta d\Delta\phi}$, as a function of $\Delta\eta$ and $\Delta\phi$ in high multiplicity ($N \geq 110$) pp events at $\sqrt{s} = 7$ TeV for $2 < p_T^{\text{trig}} < 3$ GeV/c and $1 < p_T^{\text{assoc}} < 2$ GeV/c is shown in Fig. 4a. The ridge-like structure is clearly visible. However, at higher p_T^{trig} of 5–6 GeV/c as presented in Fig. 4b, the ridge seems to almost disappear.

After projecting to one-dimensional (1-D) $\Delta\phi$ correlation functions in a limited $\Delta\eta$ range, the integrated associated yield is calculated on the near side (over the $\Delta\phi$ range from 0 to the minimum ϕ position of the distribution) for both jet ($|\Delta\eta| < 1$) and ridge ($2 < |\Delta\eta| < 4$) regions relative to the minimum of the distribution. Fig. 5 shows the multiplicity dependence of the near-side associated yield in the jet and ridge regions respectively, for the representative transverse momentum bin of $2 < p_T^{\text{trig}} < 3$ GeV/c and $1 < p_T^{\text{assoc}} < 2$ GeV/c, where the ridge effect appears to be strongest. The magnitude of the jet yield is enhanced by a factor of roughly 2–3 when

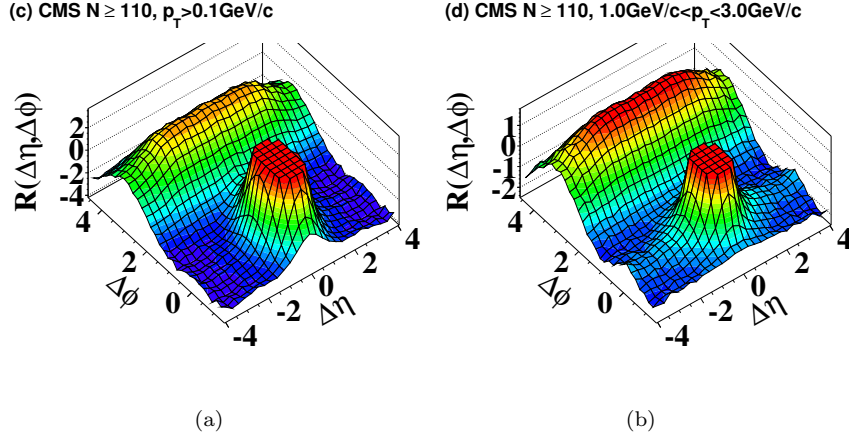


Fig. 3: 2-D dihadron correlation functions for high multiplicity ($N \geq 110$) pp collisions at $\sqrt{s} = 7$ TeV (a) with $p_T > 0.1 \text{ GeV}/c$ and (b) with $1 < p_T < 3 \text{ GeV}/c$ measured by the CMS experiment¹. The “ridge” refers to the structure in (b) that has a narrow width around $\Delta\phi = 0$ and extends over the entire $\Delta\eta$ range.

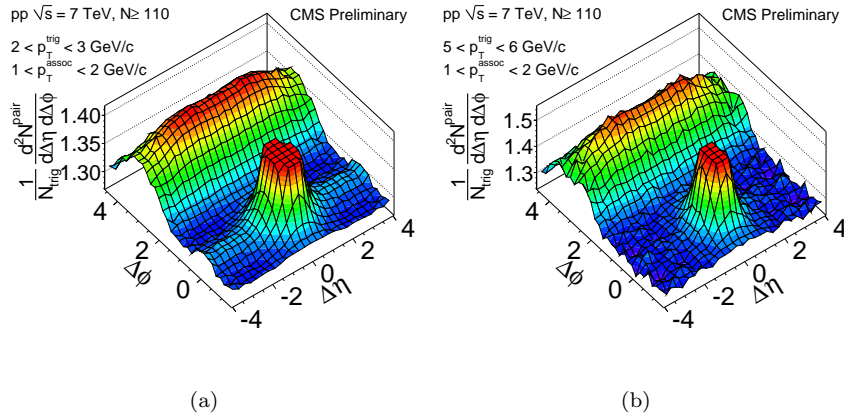


Fig. 4: 2-D per-trigger-particle associated yield distribution for charged hadrons as a function of $\Delta\eta$ and $\Delta\phi$ from high multiplicity ($N \geq 110$) pp collisions at $\sqrt{s} = 7$ TeV, for (a) $2 < p_T^{\text{trig}} < 3 \text{ GeV}/c$ and $1 < p_T^{\text{assoc}} < 2 \text{ GeV}/c$, and (b) $5 < p_T^{\text{trig}} < 6 \text{ GeV}/c$ and $1 < p_T^{\text{assoc}} < 2 \text{ GeV}/c$ measured by the CMS experiment¹⁰.

going to events that produce 10 times more multiplicity than minimum bias events. The ridge effect gradually turns on with event multiplicity around $N \sim 50 - 60$ (about four times of the average multiplicity in minimum bias events) and smoothly

increases toward the high multiplicity region. The p_T^{trig} dependence of the jet and ridge yield is shown in Figure 6 for fixed associated transverse momentum range of $1 < p_T^{\text{assoc}} < 2$ GeV/c in bins of event multiplicity. The jet yield increases with p_T^{trig} as expected due to the increasing contributions from high E_T jets. In high multiplicity events, the ridge yield first increases with p_T^{trig} , reaches a maximum around $p_T^{\text{trig}} \sim 2\text{--}3$ GeV/c and drops toward even higher p_T^{trig} .

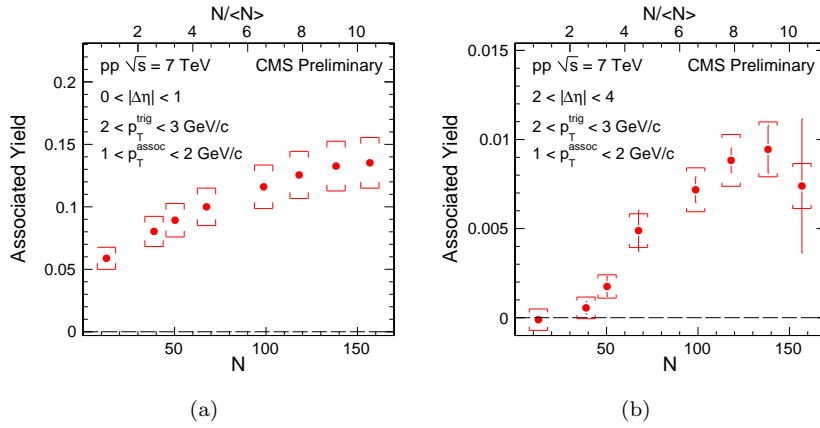


Fig. 5: Integrated associated yields of the near-side ridge in (a) the short-range jet region ($0 < |\Delta\eta| < 1$) and (b) the long-range ridge region ($2 < |\Delta\eta| < 4$), for particles with $2 < p_T^{\text{trig}} < 3$ GeV/c and $1 < p_T^{\text{assoc}} < 2$ GeV/c, as a function of event multiplicity from pp collisions at $\sqrt{s} = 7$ TeV measured by the CMS experiment ¹⁰.

3. The “Ridge” in relativistic heavy-ion collisions

Measurement of dihadron correlations is also a powerful tool in tackling many aspects of particle production in relativistic heavy ion collisions, where properties of particle correlations were found to be strongly modified in the presence of a hot and dense QGP matter. The near-side ridge structure in 2-D dihadron correlations was first observed in AuAu collisions at the center-of-mass energy per nucleon pair ($\sqrt{s_{NN}}$) of 200 GeV from the STAR experiment at RHIC ^{12,13} (Fig. 7a). Note that the ridge studied at RHIC normally refers to the residual long-range near-side correlations after subtracting the known source of correlations from hydrodynamical elliptic flow (v_2) ¹⁴. It was then extended to wider $\Delta\eta$ range up to 4 units by the PHOBOS experiment with a wider detector acceptance ¹⁵ (Fig. 7b). The properties of the ridge have been extensively studied at both RHIC, and more recently the LHC. Fig. 7c shows a representative measurement of dihadron correlations over a large phase space in 2.76 TeV PbPb collisions from the CMS experiment at the

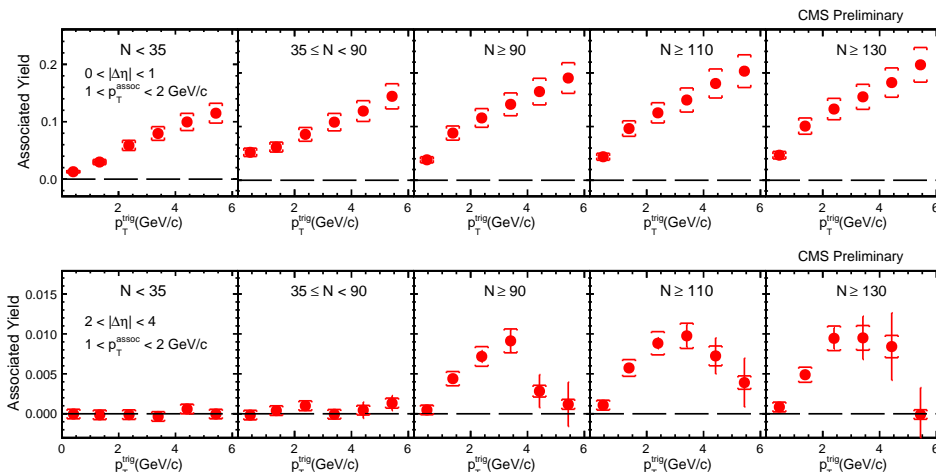


Fig. 6: Integrated associated yields of the near-side ridge in (a) the short-range jet region ($0 < |\Delta\eta| < 1$) and (b) the long-range ridge region ($2 < |\Delta\eta| < 4$), for particles with $1 < p_T^{\text{assoc}} < 2$ GeV/c, as a function of p_T^{trig} in different bins of event multiplicity from pp collisions at $\sqrt{s} = 7$ TeV¹⁰.

LHC¹⁶, where a clear and significant ridge-like structure is observed on the near side. The ridge structure has been first observed for particles with transverse momenta from several hundred MeV/c to a few GeV/c but also found recently to emerge for very high p_T (> 20 GeV/c) particles at CMS¹⁷.

Understanding of the ridge phenomena in heavy ion collisions have been evolving over the past several years. It has been qualitatively described in many different models^{18,19,20,21,22,23,24,25,26,27,28,29}, some attributing the ridge to the medium response to its interactions with high-energy partons, while others attribute the ridge to the dynamics of medium itself. Motivated by recent theoretical developments^{29,30,31,32,33}, there has been more and more evidence implying that the v_2 -subtracted residual long-range ridge effect can be understood in analogy to the elliptic flow in the context of hydrodynamics due to the initial geometric fluctuations, particularly the “triangularity”, leading to higher-order eccentricity and thus final-state azimuthal anisotropy^{29,30,31,32,33}. As a result, the long-range dihadron correlations are now commonly analyzed using the technique of Fourier harmonic decomposition^{16,34,35,36},

$$\frac{1}{N_{\text{trig}}} \frac{dN^{\text{pair}}}{d\Delta\phi} \sim \left\{ 1 + \sum_{n=1}^{\infty} 2V_{n\Delta} \cos(n\Delta\phi) \right\}, \quad (2)$$

where the Fourier coefficients, $V_{n\Delta}$, are related to the anisotropy (v_n) of final-state particle azimuthal distribution. The anisotropies for low p_T (up to 1–2 GeV/c) particles are driven by the hydrodynamic evolution, while path-length dependence of

in-medium parton energy loss is believed to be responsible for the anisotropy observed for higher p_T (> 10 GeV/ c or above) particles^{37,38,39}. Comprehensive studies of dihadron correlations over broad a range of phase space and kinematics in heavy ion collisions provide us valuable information in determining the initial conditions of the QGP matter as well as medium transport properties such as shear viscosity, opacity etc.

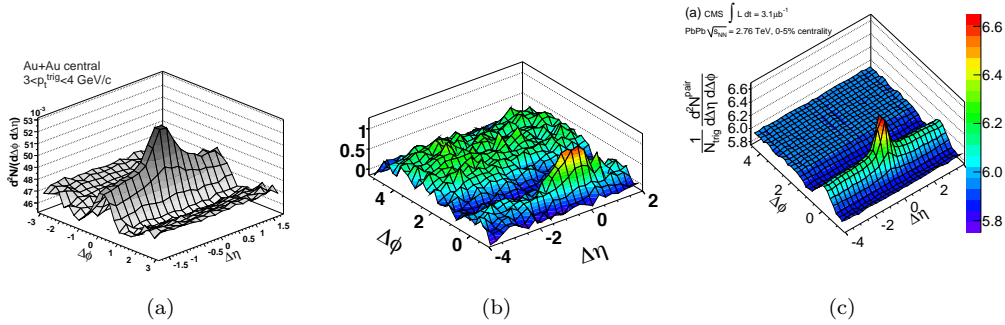


Fig. 7: 2-D dihadron correlation functions measured in (a) 200 GeV AuAu collisions by the STAR experiment¹², (b) the PHOBOS experiment¹⁵ and (c) 2.76 TeV PbPb collisions by the CMS experiment¹⁶. The p_T ranges of particles are different for (a), (b) and (c) but not specified here.

4. Theoretical interpretations of the “Ridge” in pp

The long-range rapidity correlations in pp collisions were in fact observed long time ago back to 1980s in the forward-backward multiplicity correlations⁴⁰. However, what is novel about the ridge in high multiplicity pp is that particles are produced in a correlated fashion not only over long range in rapidity but also collimated in azimuthal angle (near-side). This peculiar new feature was not observed before in pp or $p\bar{p}$, or any theoretical modelings of pp collisions.

The microscopic dynamics of high multiplicity particle production and near-side ridge correlations in pp have not been fully understood yet. Nevertheless, such high multiplicity events are likely to result from very “central” pp events (small impact parameter, or large overlapping region like the central nucleus-nucleus collisions), where multiparton interactions become more relevant^{41,42}. Furthermore, based on causality constraints of particle production as illustrated in Fig. 8 from Ref. 25, any final-state correlation over large rapidity gaps (several units) has to be established shortly after the interaction happens at proper time earlier than

$$\tau_{\text{init.}} = \tau_{\text{freeze-out}} \exp\left(-\frac{1}{2}|\Delta y|\right), \quad (3)$$

which is strongly suppressed at large rapidity gap, $|\Delta y|$ ²⁵. Here $\tau_{\text{freeze-out}}$ is the freeze-out time of particle production. An acute analogy of it is the large scale correlations and fluctuations in the cosmic microwave background (CMB). The fact that the structure of the universe today is so smooth (up to one part in 100,000) and correlated over large distances that are casually disconnected indicates the existence of a rapidly inflationary era in the very early stage of the universe. The amount of correlations and fluctuations observed in the CMB provide crucial information on the primordial quantum fluctuations, which lead to the formation of galaxies. Therefore, the observation of long-range near-side ridge correlations in pp interactions gives us an exciting opportunity to investigate the initial-state structure of the proton wavefunction, as well as the quantum fluctuations of the color field at very short timescale.

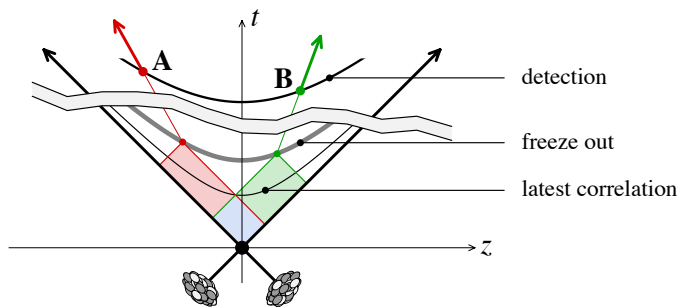


Fig. 8: Illustration of causality constraint on the long-range rapidity correlations from Ref. 25, which provides information on early time dynamics.

As already pointed out in Sec. 3, the near-side ridge phenomena in heavy ion collisions can be interpreted in terms of the hydrodynamic phenomena. The eccentricity of initial-state energy density profile in the transverse plane of the overlapping nucleus-nucleus system is propagated to the final-state particle azimuthal anisotropy via pressure driven radial flow on an event-by-event basis. Since these anisotropies are originated from the initial condition, they are boost invariant in rapidity. In dihadron angular correlations, the hydrodynamic flow effect emerges in the form of Fourier harmonic components, $\sim \cos(n\Delta\phi)$, referred to as the elliptic ($n = 2$) and higher-order ($n > 2$) flow. Each of the Fourier terms gives rise to a local maximum at $\Delta\phi = 0$ independent of $\Delta\eta$, which sums up to a ridge-like structure. In principle, a similar ridge structure should also be present on the away side ($\Delta\phi \sim \pi$) of the correlation function. However, it is often mixed up with the so-called “non-flow” correlations from dijets that are back-to-back in ϕ extending over $\Delta\eta$, thus is more complicated.

Applying the hydrodynamic approach to proton-proton collisions, it is feasible to assume that high multiplicity events are associated with very large overlap of the

initial proton wavefunctions. The density profile of the overlapping region (mostly consisting of soft gluon fields) by no means has to be smooth and isotropic. Naively speaking, an oversimplified configuration of three “hot spots” initial state from constituent quarks in a proton could generate an initial-state eccentricity event-by-event. Given the presence of final-state parton/hadron interactions (not necessarily ideal hydrodynamics with zero mean free path) in high multiplicity pp, the initial-state fluctuations would lead to a ridge-like dihadron correlation structure, similar to that in heavy-ion collisions. The observed p_T dependence of the ridge effect in high multiplicity pp (Fig. 6) shows a trend of first rise and a subsequent fall at higher p_T . This also resembles the behavior of collective flow phenomena in heavy ion collisions. Fig. 9 shows a theoretical calculation of dihadron correlations for high multiplicity pp using the EPOS model based on the hydrodynamic approach⁴³. The initial state consists of multiple color flux tubes along the longitudinal direction (identical at different rapidity), with anisotropic energy density in the transverse plane. A near-side ridge structure can be clearly seen with comparable magnitude to the experimental data in Fig. 9b, while the effect disappears if the hydrodynamic evolution is turned off in the model (Fig. 9a). More discussions of possible elliptic and higher-order flow effects in pp can be found in a series of literatures in Refs. 44, 45, 46, 47, 48, 49, 50.

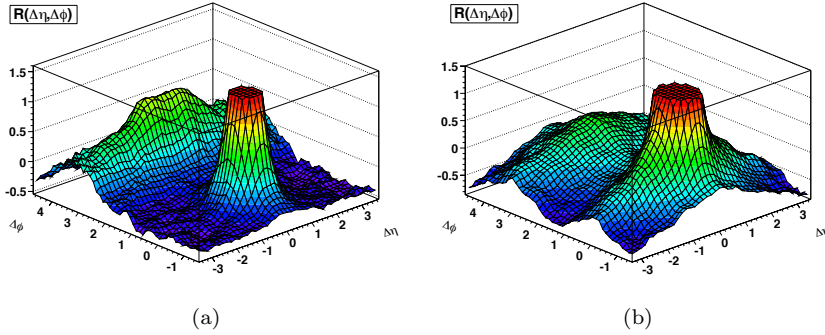


Fig. 9: 2-D dihadron correlation functions from the EPOS model for high multiplicity events in pp collisions at $\sqrt{s} = 7$ TeV (a) without hydrodynamic evolution and (b) with hydrodynamic evolution from Ref. 43. The p_T range of particles is 1–3 GeV/ c .

Motivated by the concept of gluon saturation at very small x in QCD, the theory of color glass condensate (CGC) describes the initial state of nuclear matter at very high energy^{51,52}. It employs the first principle approach of QCD and has been proved to be very successful in describing a lot of observables in high-energy nucleus-nucleus collisions. In this framework, glasma color flux tubes are

first formed, getting stretched along the longitudinal direction as the two nuclei are passing by, as illustrated in Fig. 11a. Consequently, particles produced by the glasma tubes are naturally correlated over long-range in rapidity. This aspect of the model is similar to the hydrodynamic approach presented earlier. A glasma tube has a typical size of $1/Q_S$ in the transverse direction, where Q_S is the saturation scale that grows with collision energy and centrality. The high multiplicity events in pp are expected to sample collisions that correspond to very small impact parameter (or “central” events). It was argued that the saturation scale in pp increases toward smaller impact parameter, as shown in Fig. 10 extracted from HERA data ⁵³. Once $Q_S \gg \Lambda_{QCD}$ (which is the case for high multiplicity pp events), the perturbative approach becomes valid to describe the dynamics of the glasma tubes. An example diagram of “Glasma graphs” is shown in Fig. 11b. Unlike the ridge from hydrodynamics produced by the radial flow boost, an intrinsic $\Delta\phi$ collimation of final-state hadrons is suggested by the calculations of “Glasma graphs” over long-range in rapidity ^{55,54}. The magnitude of the intrinsic ridge from the Glasma model is found to be enough to describe the experimental data. No radial flow boost is needed, in contrast to that in heavy-ion collisions. The p_T and event multiplicity dependence of the near-side ridge yield from the Glasma model in pp show an intriguing agreement with the CMS data, as shown in Fig. 12. The maximum strength of the ridge magnitude in particle p_T occurs approximately at the saturation scale, Q_S .

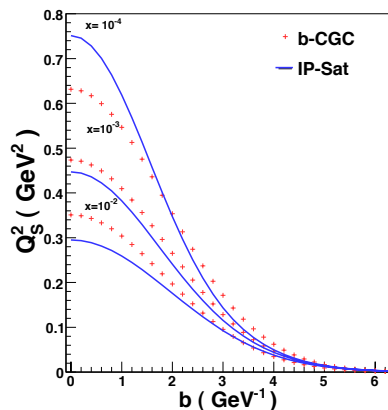


Fig. 10: The saturation scale as a function of impact parameter in pp collisions extracted from HERA data in two different saturation models ⁵³.

A third category of theoretical interpretations lies along the line of jet-induced ridge. The representative mechanisms include the energy loss of semihard partons inducing fluctuation of local soft parton density along their passage ⁵⁶; momentum kick model of QCD strings pushed by the outgoing high E_T partons ⁵⁷. These scenarios would predict that the ridge persists at very high p_T , which does not

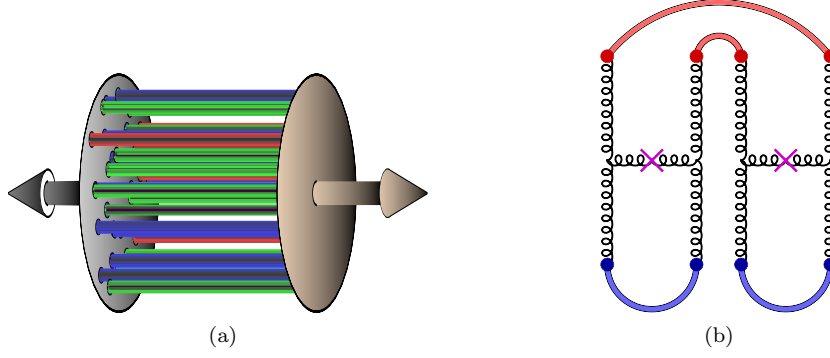


Fig. 11: (a) Glasma color flux tubes stretched between the two passing nuclei remnants with a typical transverse radius of $1/Q_S$; (b) Representative diagram of Glasma color flux tube ⁵⁴.

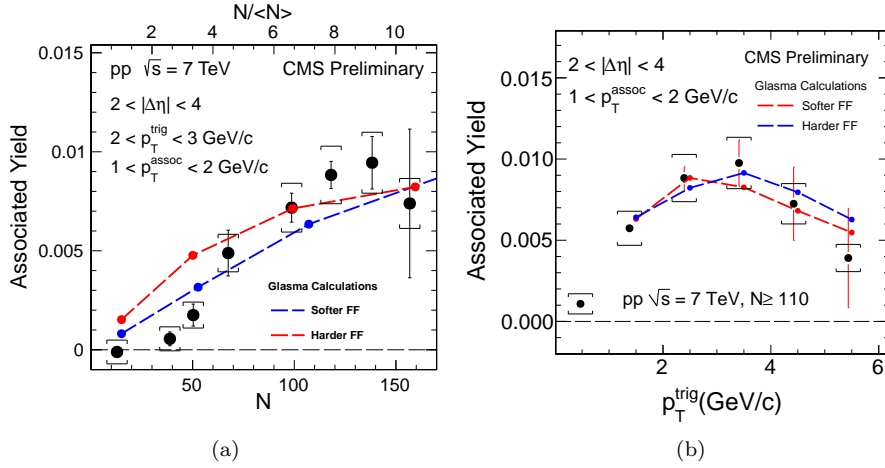


Fig. 12: Associated yield of the near-side ridge calculated from the Glasma model (a) for four different initial saturation scales corresponding to different event multiplicity and (b) as function of p_T for high multiplicity pp events ⁵⁴. Different colors of the curves correspond to softer (blue) and harder (red) fragmentation functions of the Glasma tube. Black points are data measured by the CMS experiment.

seem to be supported by the present data, although the statistical uncertainties are rather limited above $p_T \sim 6$ GeV/c. Also, as shown in Fig. 3b, the correlation structure at $\Delta\phi \sim 0$ always consists of a narrow peak in both $\Delta\eta$ and $\Delta\phi$ from jet fragmentation sitting on top of the long-range ridge in $\Delta\eta$. In CGC or hydrodynamic scenarios, jet and ridge are induced by different processes, which have no correlations

in ϕ but only brought to have the same $\Delta\phi$ by construction. On the other hand, the jet-induced ridge would always be collimated with the jet in ϕ direction of each event. Future studies of multiparticle correlations will be able to differentiate among these scenarios. The scenario of jet-induced ridge is more close to the other striking phenomena observed in heavy ion collisions, namely the “jet quenching”. In particular, a ridge correlation structure is also observed recently for trigger particle p_T as high as 20 GeV/ c in PbPb collisions at the LHC ¹⁷, where particle production must be associated with jet fragmentation. The common interpretation is the path length or initial-state geometry dependence of jet quenching effect, which generates an azimuthal anisotropic distribution also for high E_T jets but has nothing to do with hydrodynamic flow ^{63,64,65,66,67,68,69}. If a ridge signal can be observed in pp at very high p_T , it may provide intriguing evidence of jet-medium interaction, or jet quenching, in pp collisions. Future experimental results will provide us the answers.

5. Summary and Outlook of future directions

Looking into the future, the observation of long-range near-side ridge correlation in high multiplicity pp collisions opens up the opportunities of studying very high density QCD physics in a tiny system size. Although it is still too early to draw any definitive conclusion on the physical original of the observation, a non-exhaustive list of possible further studies can be proposed and carried out experimentally in future program at the LHC. Particularly, in terms of its connection to the heavy ion physics, understanding the ridge phenomena in high multiplicity pp would have direct impact on the field of relativistic heavy ion physics, and thus should be extensively explored.

In order to address this question, the general approach is to investigate a variety of key and unique heavy-ion observables in high multiplicity pp events and convey a comprehensive comparison between the two systems. While the observation of the ridge may be regarded as a first hint of collective effect in pp, its properties can be examined further via a series of topics:

- Identified hadron spectra and correlations over large rapidity range. If the flow effect is indeed present, a modification to the p_T spectra, particularly at low p_T , should be observed with a dependence on the particle species. Meanwhile, the magnitude of the flow-induced ridge with identified particles would show a mass ordering as was observed in heavy ion collisions. This will be a critical test of the hydrodynamic scenario.
- Studies of azimuthal correlations among multiple particles separated widely in rapidity would help eliminate the short-range non-flow correlations primarily from the jets ⁵⁸ and extract purer signature of collective effect. Direct extraction of flow Fourier harmonics may be realized.
- Measurements of Bose-Einstein Correlations (BEC) ⁵⁹ and heavy flavor production ⁶⁰ in high multiplicity pp from the ALICE experiment have shown very interesting behaviors. The properties of these observables can be

explored with better precision in the future and compared with theoretical predictions^{61,62,70,71}.

Furthermore, to prove the presence of jet quenching will be another crucial milestone forward to demonstrate the existence of the medium effect in high multiplicity pp collisions. The challenge lies in the difficulty of identifying an unambiguous reference since the hard probes themselves are also enhanced by requiring high multiplicity in the event. A powerful tool to use could be the rare electroweak probes like the isolated photon to calibrate the initial jet energy and study the energy distribution on the away side as a function of event multiplicity. As already mentioned in Sec. 4, inspired by the recent observation of near-side ridge for very high p_T particles in 2.76 TeV PbPb collisions by the CMS experiment at the LHC¹⁷, very high- p_T ridge in high multiplicity pp is probably the most promising, cleanest way to demonstrate the presence of jet-medium interactions in these high-density pp events.

In the high-energy collisions of protons at the LHC, we are exploring an unprecedented territory of QCD physics under extreme condition in a small collision system. Although QCD has been probed with high accuracy in the high p_T regime, its non-perturbative behavior at low p_T is still poorly understood. It is crucial to clarify the dynamics of the high multiplicity pp interactions and provide insight on studying the internal structure of the protons at much finer time and spatial scales than ever achieved before. Exciting new opportunities of discovering more surprises are awaiting us in the near future!

Acknowledgments

I would like to thank Dragos Velicanu for careful reading the manuscript and valuable suggestions.

References

1. V. Khachatryan *et al.* [CMS Collaboration], JHEP **1009** 091 (2010).
2. B. Alver *et al.* [PHOBOS Collaboration], Phys. Rev. **C83**, 024913 (2011).
3. I. Arsene *et al.* [BRAHMS Collaboration], Nucl. Phys. **A757**, 1 (2005).
4. K. Adcox *et al.* [PHENIX Collaboration], Nucl. Phys. **A757**, 184 (2005).
5. B. B. Back *et al.* [PHOBOS Collaboration], Nucl. Phys. **A757**, 28 (2005).
6. J. Adams *et al.* [STAR Collaboration], Nucl. Phys. **A757**, 102 (2005).
7. K. Eggert *et al.*, Nucl. Phys. **B86**, 201 (1975).
8. B. Alver *et al.* [PHOBOS Collaboration], Phys. Rev. **C75**, 054913 (2007).
9. B. Alver *et al.* [PHOBOS Collaboration], Phys. Rev. **C81**, 024904 (2010).
10. V. Khachatryan *et al.* [CMS Collaboration], *CMS Physics Analysis Summary HIN-11-006* (2011).
11. W. Li [CMS Collaboration], J. Phys. **G38**, 124027 (2011).
12. B. I. Abelev *et al.* [STAR Collaboration], Phys. Rev. **C80**, 064912 (2009).
13. J. Adams *et al.* [STAR Collaboration], Phys. Rev. Lett. **95**, 152301 (2005).
14. S. A. Voloshin, A. M. Poskanzer and R. Snellings, arXiv:0809.2949 [nucl-ex].

15. B. Alver *et al.* [PHOBOS Collaboration], Phys. Rev. Lett. **104**, 062301 (2010).
16. S. Chatrchyan *et al.* [CMS Collaboration], JHEP **1107**, 076 (2011).
17. S. Chatrchyan *et al.* [CMS Collaboration], arXiv:1204.1850 [nucl-ex].
18. N. Armesto, C. A. Salgado and U. A. Wiedemann, Phys. Rev. Lett. **93**, 242301 (2004).
19. A. Majumder, B. Muller and S. A. Bass, Phys. Rev. Lett. **99**, 042301 (2007).
20. C. B. Chiu and R. C. Hwa, Phys. Rev. **C72**, 034903 (2005).
21. C. -Y. Wong, Phys. Rev. **C78**, 064905 (2008).
22. S. A. Voloshin, Phys. Lett. **B632**, 490 (2006).
23. P. Romatschke, Phys. Rev. **C75**, 014901 (2007).
24. E. V. Shuryak, Phys. Rev. **C76**, 047901 (2007).
25. A. Dumitru *et al.*, Nucl. Phys. **A810**, 91 (2008).
26. S. Gavin, L. McLerran and G. Moschelli, Phys. Rev. **C79**, 051902 (2009).
27. K. Dusling, D. Fernandez-Fraile and R. Venugopalan, Nucl. Phys. **A828**, 161 (2009).
28. Y. Hama *et al.*, Nonlin. Phenom. Complex Syst. **12**, 466 (2009).
29. B. Alver and G. Roland, Phys. Rev. **C81**, 054905 (2010).
30. B. H. Alver *et al.*, Phys. Rev. **C82**, 034913 (2010).
31. B. Schenke, S. Jeon and C. Gale, Phys. Rev. Lett. **106**, 042301 (2011).
32. H. Petersen *et al.*, Phys. Rev. **C82**, 041901 (2010).
33. D. Teaney and L. Yan, Phys. Rev. **C83**, 064904 (2011).
34. S. Chatrchyan *et al.* [CMS Collaboration], arXiv:1201.3158 [nucl-ex].
35. K. Aamodt *et al.* [ALICE Collaboration], Phys. Lett. **B708**, 249 (2012).
36. G. Aad *et al.* [ATLAS Collaboration], arXiv:1203.3087 [hep-ex].
37. A. Adare *et al.* [PHENIX Collaboration], Phys. Rev. Lett. **105**, 142301 (2010).
38. G. Aad *et al.* [ATLAS Collaboration], Phys. Lett. **B707**, 330 (2012).
39. S. Chatrchyan *et al.* [CMS Collaboration], arXiv:1204.1850 [nucl-ex].
40. K. Alpgard *et al.* [UA5 Collaboration], Phys. Lett. **B123**, 361 (1983).
41. J. Casalderrey-Solana and U. A. Wiedemann, Phys. Rev. Lett. **104**, 102301 (2010).
42. M. Strikman, Acta Phys. Polon. **B42**, 2607 (2011).
43. K. Werner, I. Karpenko and T. Pierog, Phys. Rev. Lett. **106**, 122004 (2011).
44. P. Bozek, Phys. Rev. **C85**, 014911 (2012).
45. W. -T. Deng, Z. Xu and C. Greiner, Phys. Lett. **B711**, 301 (2012).
46. E. Avsar *et al.*, J. Phys. **G38**, 124053 (2011).
47. S. M. Troshin and N. E. Tyurin, Mod. Phys. Lett. **A26**, 1095 (2011).
48. A. Kisiel, Phys. Rev. **C84**, 044913 (2011).
49. P. Bozek, Eur. Phys. J. **C71**, 1530 (2011).
50. E. Avsar *et al.*, Phys. Lett. **B702**, 394 (2011).
51. E. Iancu and R. Venugopalan, In *Hwa, R.C. (ed.) et al.: Quark gluon plasma* 249-3363 [hep-ph/0303204].
52. F. Gelis *et al.*, Ann. Rev. Nucl. Part. Sci. **60**, 463 (2010).
53. R. Venugopalan, PoS ICHEP **2010**, 567 (2010).
54. K. Dusling and R. Venugopalan, arXiv:1201.2658 [hep-ph].
55. A. Dumitru *et al.*, Phys. Lett. **B697**, 21 (2011).
56. R. C. Hwa and C. B. Yang, Phys. Rev. **C83**, 024911 (2011).
57. C. -Y. Wong, Phys. Rev. **C84**, 024901 (2011).
58. J. D. Bjorken, S. J. Brodsky and A. S. Goldhaber, private communications.
59. K. Aamodt *et al.* [ALICE Collaboration], Phys. Rev. **D84**, 112004 (2011).
60. B. Abelev *et al.* [ALICE Collaboration], arXiv:1202.2816 [hep-ex].
61. K. Werner *et al.*, arXiv:1104.2405 [hep-ph].
62. C. -Y. Wong, arXiv:1112.1091 [hep-ph].
63. S. Peigne and A. V. Smilga, Phys. Usp. **52**, 659 (2009).

64. S. Wicks *et al.*, Nucl. Phys. **A784**, 426 (2007).
65. J. Jia and R. Wei, Phys. Rev. **C82**, 024902 (2010).
66. J. Jia, W. A. Horowitz and J. Liao, Phys. Rev. **C84**, 034904 (2011).
67. T. Renk, Phys. Rev. **C83**, 024908 (2011).
68. B. Betz, M. Gyulassy and G. Torrieri, Phys. Rev. **C84**, 024913 (2011).
69. B. Betz and M. Gyulassy, arXiv:1201.0281 [nucl-th].
70. S. Vogel *et al.*, Nucl. Phys. **A855**, 448 (2011).
71. F. -M. Liu and K. Werner, Phys. Rev. Lett. **106**, 242301 (2011).